

# Catalytic Transfer Hydrogenation of Furfural to Furfuryl Alcohol with Recyclable Al–Zr@Fe Mixed Oxides

Jian He,<sup>[a, b]</sup> Hu Li,<sup>[a]</sup> Anders Riisager,<sup>\*[b]</sup> and Song Yang<sup>\*[a]</sup>

A series of magnetic, acid/base bifunctional Al–Zr@Fe<sub>3</sub>O<sub>4</sub> catalysts were successfully prepared by a facile coprecipitation method and utilized in the catalytic transfer hydrogenation (CTH) of furfural to furfuryl alcohol with 2-propanol as hydrogen source. The physicochemical properties and morphologies of the as-prepared catalysts were characterized by various techniques, including XRD analysis, N<sub>2</sub> physisorption, vibrating sample magnetometry, thermal gravimetry analysis, X-ray fluorescence spectroscopy, NH<sub>3</sub>/CO<sub>2</sub> temperature-programmed desorption, SEM, and TEM. The Al<sub>7</sub>Zr<sub>3</sub>@Fe<sub>3</sub>O<sub>4</sub>(1/1) catalyst with a

Al<sup>3+</sup>/Zr<sup>4+</sup>/Fe<sub>3</sub>O<sub>4</sub> molar ratio of 21:9:3 was found to exhibit a high furfuryl alcohol yield of 90.5% in the CTH from furfural at 180 °C after 4 h with a comparatively low activation energy of 45.3 kJ mol<sup>-1</sup>, as calculated from the Arrhenius equation. Moreover, leaching and recyclability tests confirmed Al<sub>7</sub>Zr<sub>3</sub>@Fe<sub>3</sub>O<sub>4</sub>(1/1) to function as a heterogeneous catalyst that could be reused for at least five consecutive reaction runs without significant loss of catalytic activity after simple recovery by an external magnet. Notably, the catalyst proved also efficient for hydrogenation of other biomass-derived furanic aldehydes.

## Introduction

Catalytic upgrading of biomass-derived platform compounds to fuels and value-added chemicals are attracting more and more attention, because abundant biomass is a sustainable organic carbon resource and regarded as a promising alternative to traditional fossil resources for producing fuels and chemicals.<sup>[1–5]</sup> Furfural (FF), as an important platform compound, is obtainable from hemicellulose (one of the main components of lignocellulose) through an acid-catalyzed hydrolysis and dehydration process. Owing to the highly functionalized molecular structure of FF (i.e., C–O, C=C, and C=O groups) it can serve as an ideal feedstock for the synthesis of various biofuels and value-added chemicals through different conversion reactions, such as hydrogenation, oxidation, hydrogenolysis, aldolization, and aldol condensation.<sup>[6,7]</sup> Particularly, hydrogenation or hydrogenolysis of FF has received immense attention because many important industrial chemicals and biofuel additives are obtainable directly from FF, such as furfuryl alcohol

(FAOL), tetrahydrofurfuryl alcohol (THFAOL), 2-methylfuran (2-MF), and 2-methyltetrahydrofuran (2-MTHF).<sup>[8]</sup> As one of the most important derivatives, FAOL has been widely applied as a versatile raw material for the industrial synthesis of fine chemicals including resins, lubricants, fibers, adhesives, vitamin C, and lysine.<sup>[9,10]</sup> Additionally, important furanic downstream products such as levulinic acid and  $\gamma$ -valerolactone (GVL) can be obtained through FAOL after additional conversion.<sup>[11]</sup> Consequently, the design of efficient catalytic systems for the synthesis of FAOL from FF remains to be of high importance.

An efficient strategy for the production of FAOL from FF has been developed involving molecular hydrogen as H donor in the presence of supported zero-valent noble or nonnoble metal-based catalysts (e.g., Au, Pd, Ru, and Cu).<sup>[12–16]</sup> However, the high preparation cost of H<sub>2</sub> (usually prepared from fossil-based resources) and metal catalysts (often reduced under H<sub>2</sub>) as well as the flammable and explosive nature of the gas encourage exploration of alternative methods. On this basis, catalytic transfer hydrogenation (CTH) utilizing alternative H donors, such as formic acid and alcohols, has recently been proposed as an attractive way to hydrogenate organic molecules including biomass-derived compounds.<sup>[17–19]</sup> Employing abundant alcohols for the CTH process with the advantage of high selectivity towards reduction of carbonyl groups to alcoholic hydroxyl groups through the Meerwein-Ponndorf-Verley (MPV) reduction seems more appealing than the use of corrosive formic acid.<sup>[20,21]</sup> Many Lewis acid-containing/base-containing or acid/base bifunctional heterogeneous catalysts have been developed for the highly efficient synthesis of GVL from biomass-derived levulinic acid/levulinic ester by CTH using H donor alcohols<sup>[22–26]</sup> with the Lewis acid/base sites as crucial sites for the MPV reduction.<sup>[27]</sup> Very recently, several other catalysts including Hf-Beta,<sup>[28]</sup> nitrogen-doped carbon-supported

[a] J. He, Dr. H. Li, Prof. S. Yang  
State Key Laboratory Breeding Base of  
Green Pesticide & Agricultural Bioengineering,  
Key Laboratory of Green Pesticide & Agricultural Bioengineering,  
Ministry of Education, State-Local Joint Laboratory for  
Comprehensive Utilization of Biomass,  
Center for Research & Development of Fine Chemicals  
Guizhou University  
Guiyang 550025 (P.R. China)  
E-mail: yangsdqj@126.com

[b] J. He, Prof. A. Riisager  
Centre for Catalysis and Sustainable Chemistry, Department of Chemistry  
Technical University of Denmark  
DK-2800 Kgs. Lyngby (Denmark)  
E-mail: ar@kemi.dtu.dk

Supporting information and the ORCID identification number(s) for the author(s) of this article can be found under:  
<https://doi.org/10.1002/cctc.201701266>.

iron (Fe-L1/C-800),<sup>[29]</sup> and Co-Ru/C<sup>[30]</sup> have also been used as efficient solid catalysts for CTH of FF to FAOL with alcohols. Similarly, we have shown that a mesoporous organotriphosphate–zirconium nanohybrid (ZrPN) catalyst with Lewis acid/base sites efficiently catalyzed the production of FAOL from FF in 2-propanol through CTH.<sup>[31]</sup> Despite these pioneering works, it remains a much-sought-after goal to develop more efficient and lower cost heterogeneous catalysts for FAOL production by CTH.

Low-cost, mixed-metal oxides are widely applied in catalysis with renewables because of their tunable physicochemical properties closely related to catalytic activity, for example, surface area, pore size distribution, and acid/base character.<sup>[32]</sup> For instance, W–Zr mixed oxides can efficiently convert cellulose to lactic acid,<sup>[33]</sup> ethyl lactate can efficiently be obtained from triose sugars over Sn/Al oxide,<sup>[34]</sup> and glucose can (through fructose) be dehydrated into 5-hydroxymethylfurfural with Nb-doped WO<sub>3</sub>.<sup>[35]</sup> In our previous work, Al–Zr mixed oxide was confirmed to be an efficient catalyst for the production of GVL from ethyl levulinate,<sup>[23]</sup> and in continuation of our research on CTH of biomass-derived chemicals, we expected also such catalysts to be active in CTH of FF to FAOL. Solid materials with magnetic properties are highly interesting catalyst supports because they allow easy catalyst separation and recycling from liquid reaction mixtures by applying an external magnetic field. This renders the operation of such catalytic systems time-saving and energy-efficient compared to traditional filtration and centrifugation operations.<sup>[36,37]</sup> In this regard, the design and preparation of a magnetic catalyst could be highly desirable for the large-scale practical application of CTH of FF to FAOL. Accordingly, we prepared herein a series of acid/base bifunctional magnetic Al<sub>7</sub>Zr<sub>3</sub>@Fe<sub>3</sub>O<sub>4</sub> oxide catalysts by a facile coprecipitation method and explore their application in the CTH of FF to FAOL through MPV reduction using 2-propanol as H donor.

## Results and Discussion

### Characterization of catalysts

The XRD patterns of the as-prepared catalysts are depicted in Figure 1a. The Al<sub>7</sub>Zr<sub>3</sub> exhibited an amorphous nature with no clear diffraction peaks detected consistent with our previous report.<sup>[23]</sup> With regard to Fe<sub>3</sub>O<sub>4</sub>, five diffraction peaks at 30.3, 35.6, 43.3, 57.2, and 62.9° were clearly observed and assigned to the (220), (311), (400), (511), and (440) crystalline planes of Fe<sub>3</sub>O<sub>4</sub>.<sup>[38]</sup> In the case of the as-prepared Al<sub>7</sub>Zr<sub>3</sub>@Fe<sub>3</sub>O<sub>4</sub> catalysts, the Al–Zr mixed oxides remained amorphous in nature, and no additional diffraction peaks emerged indicating that no other crystal phases were generated.

The N<sub>2</sub> adsorption–desorption isotherms of the as-prepared catalysts are displayed in Figure 1b; all are type-IV isotherms with typical H3 hysteresis loop. In addition, all catalysts exhibited a relative narrow pore distribution (Figure S1 in the Supporting Information) revealing that the catalysts possessed irregular mesoporous structures. Data on surface areas and mean pore sizes obtained from BET and BJH methods,

respectively, are compiled in Table 1. The surface areas of the as-prepared catalysts slightly decreased with the increment of Fe<sub>3</sub>O<sub>4</sub> content (Table 1, entries 1–4), whereas the mean pore sizes of the materials were all around 4 nm. Furthermore, the actual element compositions of Al, Zr, and Fe in the catalysts were close to the controlled molar ratios as verified from X-ray fluorescence (XRF) measurements (entries 2–4). Thermogravimetric analysis of the Al<sub>7</sub>Zr<sub>3</sub>@Fe<sub>3</sub>O<sub>4</sub>(1/1) catalyst (Figure S2) revealed a total weight loss of 8.4% resulting from removal of physical adsorbed water (4.0%;  $T \leq 200^\circ\text{C}$ ) and remaining hydroxyl groups ( $\approx 4.4\%$ ;  $T \geq 300^\circ\text{C}$ ) for the material.<sup>[23]</sup>

The magnetic properties of the as-prepared catalysts were confirmed by measurement on a vibrating sample magnetometer (VSM). The results in Figure 1c show some superparamagnetic property of the AlZr@Fe catalysts attributed to the absence of coactivity, and the saturation magnetization values of Al<sub>7</sub>Zr<sub>3</sub>@Fe<sub>3</sub>O<sub>4</sub>(2/1), Al<sub>7</sub>Zr<sub>3</sub>@Fe<sub>3</sub>O<sub>4</sub>(1/1), and Al<sub>7</sub>Zr<sub>3</sub>@Fe<sub>3</sub>O<sub>4</sub>(1/2) were evaluated to be 6.8, 9.4, and 19.2 emu g<sup>-1</sup>, respectively, which increased with the increment of Fe<sub>3</sub>O<sub>4</sub> content (as expected).

The acid/base properties of the as-prepared materials were evaluated by NH<sub>3</sub>/CO<sub>2</sub> temperature-programmed desorption (TPD) measurements as well (Figures 1d,e and Figures S3 and S4). Considering that the materials were calcined at 300 °C and the apparent weight loss emerging at higher temperature (i.e., over 300 °C, Figure S2), the highest desorption temperature for NH<sub>3</sub> or CO<sub>2</sub> were set at 300 °C during the TPD measurement (Figures 1d). As expected, the as-prepared catalysts possessed both acid and base sites mainly originating from Al–Zr with less contribution from the Fe<sub>3</sub>O<sub>4</sub> (Table 1, entries 1–5).

The microstructure of the Al<sub>7</sub>Zr<sub>3</sub>@Fe<sub>3</sub>O<sub>4</sub>(1/1) catalyst were characterized by electron microscopy. As revealed from elemental mapping by high-angle annular dark-field scanning transmission electron microscopy (HAADF–STEM, Figure 2b) the aluminum, zirconium, iron, and oxygen elements were confirmed to be homogeneously distributed in the catalyst matrix consisting of individual particles with a size of approximately 10 nm (Figure 2c). In addition, it seemed as the Al–Zr mixed oxides with amorphous nature encapsulated the magnetic Fe<sub>3</sub>O<sub>4</sub> particles like a shell without the presence of larger bulk Al–Zr oxide particles, as presented in Figure 2d. Furthermore, the crystal faces of Fe<sub>3</sub>O<sub>4</sub> were clearly observed in the high-resolution (HR) TEM image (Figure 2e), both observations in good consistency with the results from XRD analysis (Figure 1a).

### Catalyst screening for CTH of furfural to furfuryl alcohol

The catalytic results of CTH of FF to FAOL in 2-propanol at low FF conversion (i.e., 120 °C, 0.5 h) obtained with the as-prepared Al<sub>7</sub>Zr<sub>3</sub>@Fe<sub>3</sub>O<sub>4</sub> catalysts are shown in Table 2. As expected, almost no FF conversion and FAOL product was detected if the reaction was conducted without any catalyst or in the presence of Fe<sub>3</sub>O<sub>4</sub> only (Table 2, entries 1 and 6). In contrast, relative high FAOL yield (7.5%) and formation rate (125.0 μmol g<sup>-1</sup> min<sup>-1</sup>) was found for the Al<sub>7</sub>Zr<sub>3</sub> catalyst (entry 2), indicating that the Al–Zr mixed oxides provided the main activity sites. Specifically, Al<sub>7</sub>Zr<sub>3</sub>@Fe<sub>3</sub>O<sub>4</sub>(1/2) through Al<sub>7</sub>Zr<sub>3</sub>

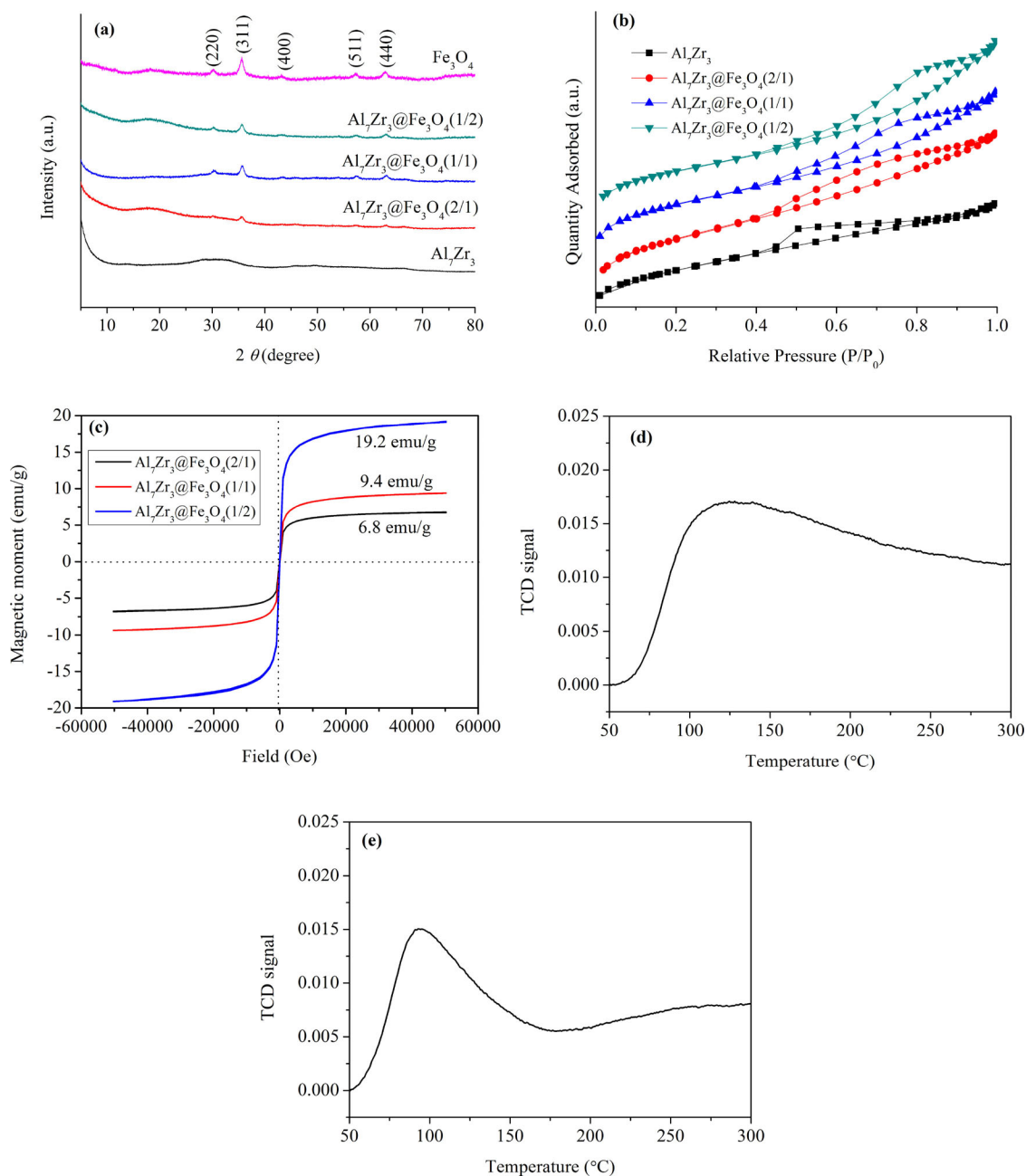


**Figure 1.** (a) XRD patterns of the as-prepared  $\text{Al}_7\text{Zr}_3$ ,  $\text{Fe}_3\text{O}_4$  and  $\text{Al}_7\text{Zr}_3@Fe_3O_4$  catalysts, (b)  $\text{N}_2$  adsorption–desorption isotherms of the as-prepared  $\text{Al}_7\text{Zr}_3@Fe_3O_4$  catalysts, (c) magnetization curves of the  $\text{Al}_7\text{Zr}_3@Fe_3O_4$  catalysts, (d)  $\text{NH}_3$ -TPD profile of  $\text{Al}_7\text{Zr}_3@Fe_3O_4(1/1)$  catalyst, and (e)  $\text{CO}_2$ -TPD profile of  $\text{Al}_7\text{Zr}_3@Fe_3O_4(1/1)$  catalyst.

Table 1. Physicochemical properties of the as-prepared catalysts						
Entry	Catalyst	BET surface area <sup>[a]</sup> [ $\text{cm}^2\text{g}^{-1}$ ]	Mean pore size <sup>[b]</sup> [nm]	Acid/base amount <sup>[c]</sup> [ $\text{mmol g}^{-1}$ ]	Al/Zr/Fe (mole ratio)	
					Controlled	Measured <sup>[d]</sup>
1	$\text{Al}_7\text{Zr}_3$	199.8	3.90	1.10/0.13	–	–
2	$\text{Al}_7\text{Zr}_3@Fe_3O_4(2/1)$	193.9	3.88	0.70/0.12	4.7:2:1	4.9:1.9:1
3	$\text{Al}_7\text{Zr}_3@Fe_3O_4(1/1)$	186.3	4.10	0.68/0.11	2.3:1:1	2.5:0.9:1
4	$\text{Al}_7\text{Zr}_3@Fe_3O_4(1/2)$	175.5	4.32	0.61/0.08	1.2:0.5:1	1.4:0.4:1
5	$\text{Fe}_3\text{O}_4$	–	–	0.2/0.03	–	–

[a] BET surface areas determined by  $\text{N}_2$  adsorption–desorption measurements. [b] Calculated by the Barrett–Joyner–Halenda method. [c] Evaluated by  $\text{NH}_3/\text{CO}_2$ -TPD method. [d] Determined by XRF analysis.

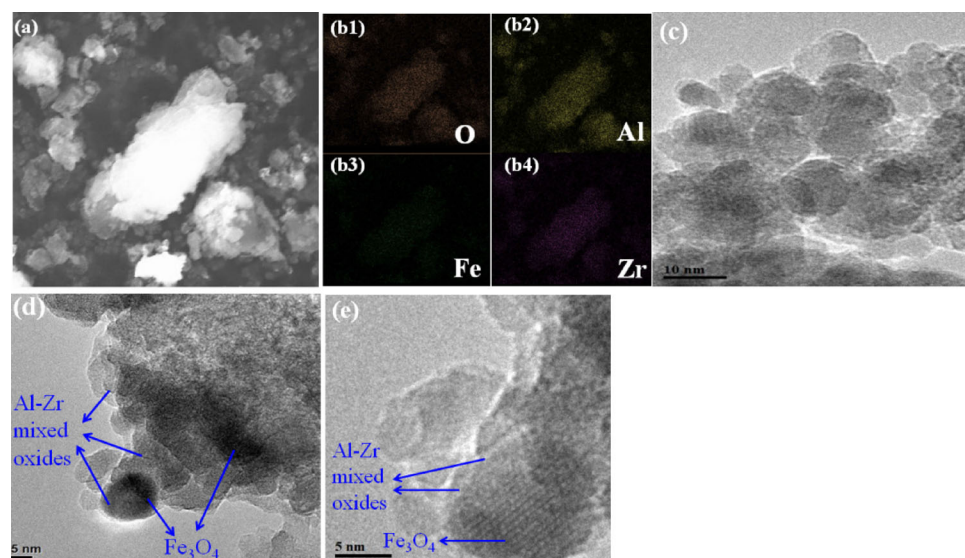


**Figure 2.** (a) HAADF-STEM image of  $\text{Al}_7\text{Zr}_3@Fe_3O_4(1/1)$ , (b) EDX elemental mappings of the  $\text{Al}_7\text{Zr}_3@Fe_3O_4(1/1)$  particle shown in (a), and (c)–(e) TEM images of  $\text{Al}_7\text{Zr}_3@Fe_3O_4(1/1)$ .

Entry	Catalyst	FF conv. [%]	FAOL yield [%]	FAOL select. [%]	FAOL formation rate [ $\mu\text{mol g}^{-1} \text{min}^{-1}$ ] <sup>[b]</sup>
1	none	1.4	0	0	0
2	$\text{Al}_7\text{Zr}_3$	21.9	7.5	34.2	125.0
3	$\text{Al}_7\text{Zr}_3@Fe_3O_4(2/1)$	16.8	6.3	37.5	105.0
4	$\text{Al}_7\text{Zr}_3@Fe_3O_4(1/1)$	7.8	5.2	66.7	86.7
5	$\text{Al}_7\text{Zr}_3@Fe_3O_4(1/2)$	7.6	4.2	55.3	70.0
6	$Fe_3O_4$	1.9	0.9	47.4	15.0

[a] Reaction conditions: FF (0.1922 g, 2 mmol), catalyst (0.04 g), 2-propanol (10 mL), 120 °C, 0.5 h. [b] Calculated as: mole of FAOL per 30 min per mass of catalyst.

exhibited a gradual increase in the FAOL formation rate rather than a linear relationship as a function of the acid or base amount (Figure S6), implying that specific acid/base sites in the catalysts played a key role in the CTH of FF through MPV reduction.<sup>[23]</sup> However, only 34.2% FAOL selectivity was observed over the  $\text{Al}_7\text{Zr}_3$  catalyst, and much acetalization product of FF with 2-propanol (i.e., 2-(diisopropoxymethyl)furan, DIPMF) formed in the reaction mixture as demonstrated by GC-MS analysis (Figure S5). This is because the acetalization of FF with alcohol is facilitated by acid sites,<sup>[39]</sup> which the  $\text{Al}_7\text{Zr}_3$  catalyst contained to the largest degree of the prepared catalysts (Table 1, entry 1). Interestingly, the introduction of  $Fe_3O_4$  as catalyst support not only rendered the catalysts magnetic, but it apparently also resulted in catalysts with improved FAOL selectivity (Table 2, entries 2–5). However, despite  $\text{Al}_7\text{Zr}_3@Fe_3O_4(1/2)$  exhibited the highest saturation magnetization ( $19.2 \text{ emu g}^{-1}$ ) among the as-prepared  $\text{Al}_7\text{Zr}_3@Fe_3O_4$  catalysts it gave the lowest FAOL yield (4.2%) and FAOL formation rate ( $70.0 \mu\text{mol g}^{-1} \text{min}^{-1}$ , entry 5), which probably resulted from its relatively low amount of acid/base sites ( $0.61/0.08 \text{ mmol g}^{-1}$ ) and relatively small specific surface area ( $175.5 \text{ m}^2 \text{ g}^{-1}$ ). In contrast, a higher FAOL yield (5.2%) and a relatively high FAOL selectivity (66.7%) were achieved with

$\text{Al}_7\text{Zr}_3@Fe_3O_4(1/1)$  (Table 2, entry 3), possibly owing to its appropriate amounts of acid/base sites ( $0.68/0.11 \text{ mmol g}^{-1}$ ) and relatively high specific surface area ( $186.3 \text{ m}^2 \text{ g}^{-1}$ ). As the  $\text{Al}_7\text{Zr}_3@Fe_3O_4(1/1)$  catalyst also had an acceptable saturation magnetization ( $9.4 \text{ emu g}^{-1}$ ), this catalyst was selected for the following studies.

### Effect of reaction temperature and time

The influence of reaction temperature and time on the CTH of FF to FAOL over  $\text{Al}_7\text{Zr}_3@Fe_3O_4(1/1)$  catalyst was investigated in detail and the results are compiled in Figure 3. Clearly, the temperature played an important role in the reaction. For example, only 15% FF conversion with 12.6% FAOL yield was obtained if the reaction was conducted at 120 °C for 1 h, whereas 65.2% yield of FAOL at 69.8% FF conversion could be attained if the reaction temperature was increased to 180 °C within a reaction time of 1 h. Moreover, it was established that relatively lower FAOL selectivity was obtained at low temperature (i.e., 120 and 140 °C) whereas high temperature (i.e., 160 and 180 °C) improved the FAOL selectivity (Figure S7). This outcome can be elucidated as resulting from the competitive acetalization of FF with 2-propanol forming DIPMF, which at low

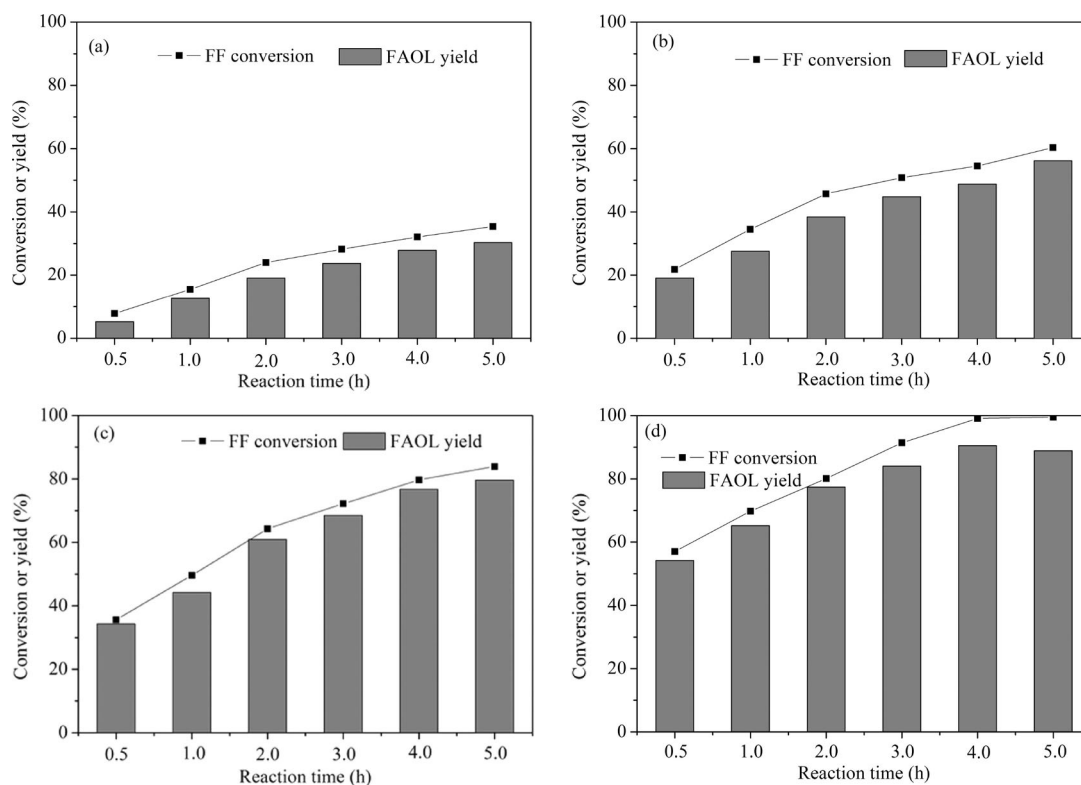


**Figure 3.** Synthesis of FAOL from FF by CTH over  $\text{Al}_7\text{Zr}_3@Fe_3O_4(1/1)$  at (a) 120 °C, (b) 140 °C, (c) 160 °C, and (d) 180 °C from 0.5 to 5 h. Reaction conditions: FF (0.1922 g, 2 mmol), catalyst (0.04 g), 2-propanol (10 mL).

reaction temperature will be more pronounced than at higher temperature because the reaction is reversible. Additionally, the reaction time also had a large influence on the reaction. Prolonging the reaction time to 4 h at 180 °C gave nearly full conversion of FF (99.1%) and 90.5% yield of FAOL. Nevertheless, the FAOL yield decreased slightly to 88.9% after extending the reaction time to 5 h at 180 °C, which resulted from the etherification of the generated FAOL with 2-propanol forming 2-isopropoxyfuran (IPF). Based on these observations, the optimal reaction temperature and time for the reaction were set as 180 °C and 4 h, respectively.

#### Effect of catalyst dosage and leaching experiments

The influence of  $\text{Al}_7\text{Zr}_3@Fe_3O_4(1/1)$  catalyst dosage on the FAOL yield of the reaction at 180 °C and 4 h was also studied. As given in Figure 4a, the blank experiment resulted in 23.5% FF conversion with only 3.6% yield of FAOL, while the main product was the acetalization product DIPMF (verified by GC-MS analysis), implying that the CTH process hardly took place without any catalyst. In contrast, the FF conversion and FAOL yield increased with the increment of the amount of catalyst (i.e., with more active sites available) reaching maximum FAOL yield (90.5%) with 0.04 g  $\text{Al}_7\text{Zr}_3@Fe_3O_4(1/1)$ . Further increase in catalyst amount (i.e., 0.06 g) lead to lower FAOL yield, which is primarily attributed to the occurrence of more side reaction, wherein the amounts of byproducts such as IPF, 4-(furan-2-yl)but-3-en-2-one (FB), and 4-(furan-2-yl)-4-hydroxybutan-2-one (FHB, Scheme 1) were enhanced in the reaction mixture as

displayed from GC-MS spectra (Figure S8). Based on the above observations the possible reaction pathways shown in Scheme 1 can be inferred for FAOL and byproducts formation from FF (IPF, FHB, FB) in the catalytic system.

To confirm the heterogeneous catalytic nature of  $\text{Al}_7\text{Zr}_3@Fe_3O_4(1/1)$  during the reaction, a filtration experiment was performed. In this case, the solid catalyst was removed from the reaction solution after 1 h with the help of an external magnet, and the solution was subsequently allowed to react for another 4 h under identical reaction condition. The results in Figure 4b show that no further FAOL formation occurred in the absence of  $\text{Al}_7\text{Zr}_3@Fe_3O_4(1/1)$ . Moreover, the filtrate was subsequently subjected to inductively coupled plasma optical emission spectroscopy (ICP-OES), and only low concentrations of Al ( $\approx 2$  ppm), Zr ( $\approx 2$  ppm), and Fe ( $< 0.2$  ppm) were measured, which did not contribute to FAOL formation (Figure 4b). This further implies that the reaction proceeded by heterogeneous catalysis.

#### Kinetic studies

To obtain more insight into the CTH of FF to FAOL over the  $\text{Al}_7\text{Zr}_3@Fe_3O_4(1/1)$  catalyst, its kinetics was investigated at four different reaction temperatures (i.e., 120, 140, 160, and 180 °C) assuming the FF conversion to be a first-order reaction. As compiled in Figure 5a, reaction rate constants ( $k$ ) were evaluated at each temperature from the corresponding slope of the plots, and the apparent activation energy ( $E_a$ ) determined to be 45.3 kJ mol<sup>-1</sup> from the corresponding Arrhenius plot

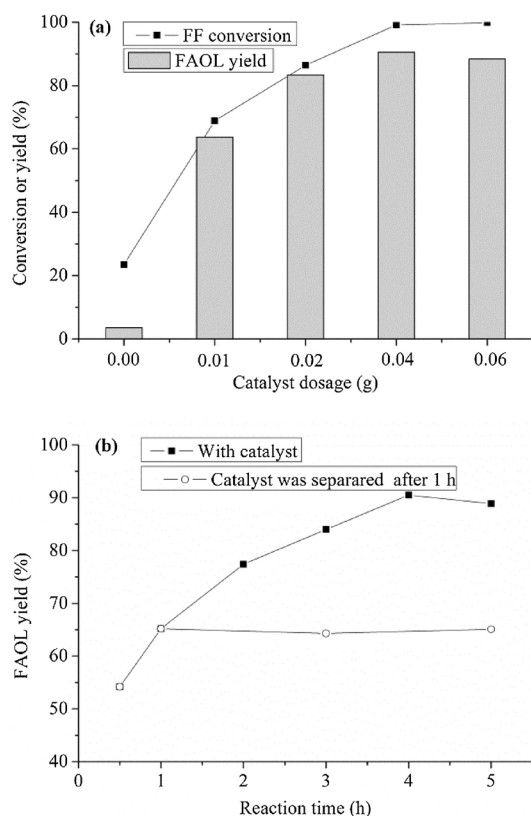
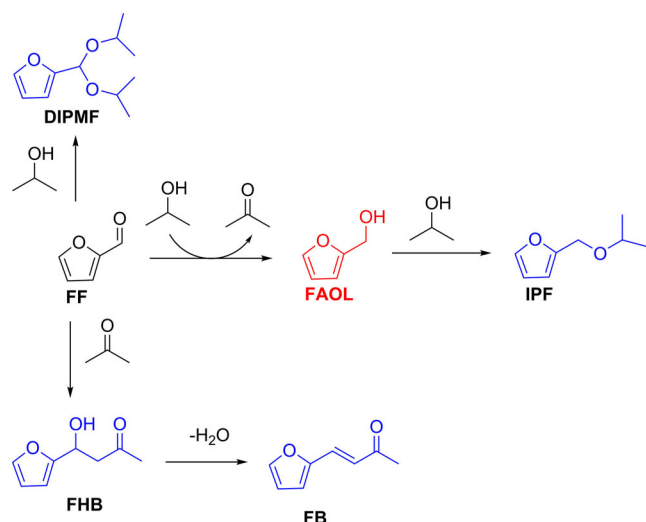


**Figure 4.** (a) Effect of  $\text{Al}_7\text{Zr}_3@Fe_3O_4(1/1)$  catalyst dosage on the production of FAOL from FF. Reaction conditions: FF (0.1922 g, 2 mmol), 2-propanol (10 mL), 180 °C, 4 h. (b) FAOL yield profiles of the reaction solution with  $\text{Al}_7\text{Zr}_3@Fe_3O_4(1/1)$  catalyst or without  $\text{Al}_7\text{Zr}_3@Fe_3O_4(1/1)$  catalyst (separated by a magnet after 1 h). Reaction conditions: FF (0.1922 g, 2 mmol), 2-propanol (10 mL),  $\text{Al}_7\text{Zr}_3@Fe_3O_4(1/1)$  (0.04 g), 180 °C.



**Scheme 1.** Possible reaction pathways for the formation of (furfuryl alcohol) FAOL and byproducts from FF.

presented in Figure 5b. This  $E_a$  value is slightly lower than those of other reported heterogeneous catalysts for the production of FAOL from FF with CTH using alcohols as H donors, and more comparable to those of metal-based catalysts using

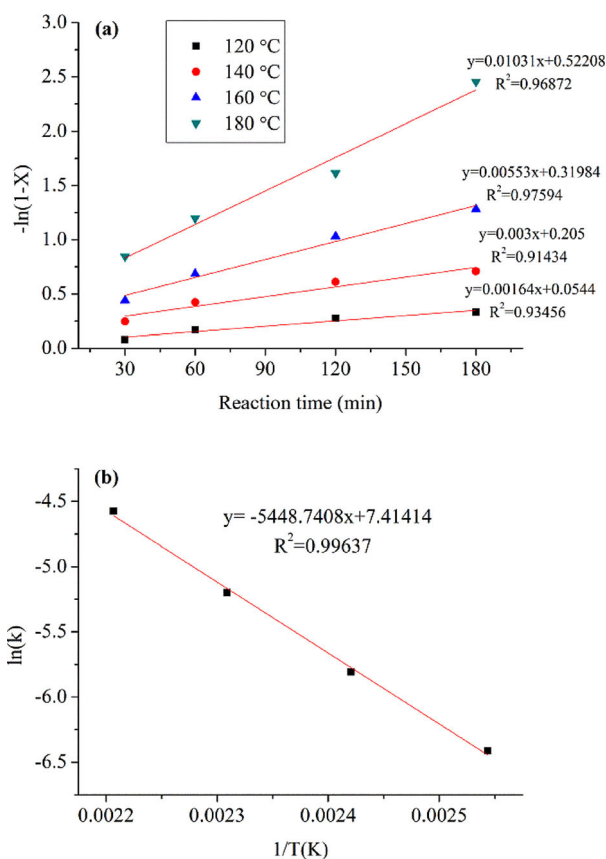


**Figure 5.** (a) Kinetic profiles of the FF to FAOL conversion by the  $\text{Al}_7\text{Zr}_3@Fe_3O_4(1/1)$  catalyst (X, FF conversion) and (b) Arrhenius plot of formation of FAOL from FF.

$\text{H}_2$  as H donor (Table S2). This further confirms the excellent catalytic property of the  $\text{Al}_7\text{Zr}_3@Fe_3O_4(1/1)$  catalyst.

### Catalyst recyclability

The reusability of the  $\text{Al}_7\text{Zr}_3@Fe_3O_4(1/1)$  catalyst in the CTH of FF to FAOL was evaluated under optimized reaction conditions (i.e., 180 °C and 4 h). In the reusability tests, the  $\text{Al}_7\text{Zr}_3@Fe_3O_4(1/1)$  catalyst was separated by an external magnet after each run, washed with ethanol and acetone twice ( $2 \times 5$  mL), dried at 80 °C for 2 h, and then directly used for the next run. The results in Figure 6 demonstrate that the catalytic activity of the catalyst decreased gradually through five consecutive reaction runs resulting in 95.9% FF conversion and 83.8% FAOL yield in the fifth reaction run.

The XRD pattern of the used catalyst after five reaction runs exhibited no clear crystallographic changes compared to the fresh catalyst (Figure 7a), and both catalyst mesoporosity (Figure 7b) as well as acid/base properties (Figure S9) also remained largely unchanged. Additionally, ICP-OES analysis demonstrated that the filtrate only contained approximately 2 ppm of Al, 3 ppm of Zr, and  $<0.2$  ppm of Fe (detection limit) after reaction for 4 h at 180 °C, indicating a very low degree of leaching of activity species into the reaction mixture. In contrast, the surface area of the used catalyst declined 15% (to

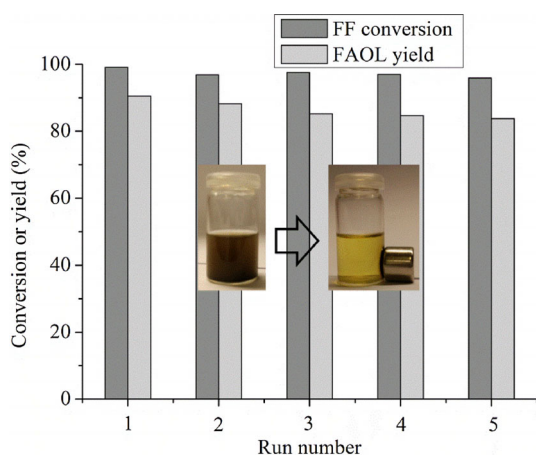


**Figure 6.** Recyclability of  $\text{Al}_7\text{Zr}_3@Fe_3O_4(1/1)$  in the synthesis of FAOL from FF. Reaction conditions: FF (0.1922 g, 2 mmol), 2-propanol (10 mL),  $\text{Al}_7\text{Zr}_3@Fe_3O_4(1/1)$  (0.04 g), 180 °C, 4 h.

$159.2\text{ m}^2\text{g}^{-1}$ ). In combination with a larger weight loss in thermal gravimetry analysis (TGA, Figure 7c), this suggests that carbon residues deposited on the catalyst during reaction, which could also explain the slight decline observed in FAOL yield during the reuse.

### Substrate scope

Biomass-derived furanic aldehydes besides FF, such as 5-hydroxymethylfurfural (HMF), 5-methylfurfural, and 2,5-diformylfuran, are also recognized as important platform chemicals and, therefore, relevant substrates for CTH. Accordingly, the feasibility of the  $\text{Al}_7\text{Zr}_3@Fe_3O_4(1/1)$  catalyst for CTH with these substrates was also examined with 2-propanol as H donor, and the results are summarized in Table 3. Clearly, the developed  $\text{Al}_7\text{Zr}_3@Fe_3O_4(1/1)$  catalyst exhibited also good catalytic performance for the alternative furanic aldehydes resulting in more than 70% yield of the corresponding products along with a considerable amount of the corresponding etherification products (not quantified). This clearly suggests the  $\text{Al}_7\text{Zr}_3@Fe_3O_4(1/1)$  catalyst to be a highly versatile catalyst for CTH of biomass-derived furanic aldehydes in general.

### Conclusions

Low-cost, magnetic acid/base bifunctional  $\text{Al}_7\text{Zr}_3@Fe_3O_4$  catalysts were prepared by a facile coprecipitation method, physicochemically characterized, and demonstrated to be efficient catalysts for the catalytic transfer hydrogenation (CTH) of furfural (FF) to furfuryl alcohol (FAOL) by using 2-propanol as H-donor. Under optimized reaction conditions (180 °C, 4 h) 99.1% conversion of FF with 90.5% yield of FAOL was achieved in the presence of  $\text{Al}_7\text{Zr}_3@Fe_3O_4(1/1)$ . The apparent activation energy of the CTH of FF to FAOL over  $\text{Al}_7\text{Zr}_3@Fe_3O_4(1/1)$  was found to be  $45.3\text{ kJ mol}^{-1}$ , which was lower than activation energies of comparable catalyst systems previously reported. Filtration experiments confirmed that the CTH reaction proceeded in a heterogeneous manner allowing the  $\text{Al}_7\text{Zr}_3@Fe_3O_4(1/1)$  catalyst to

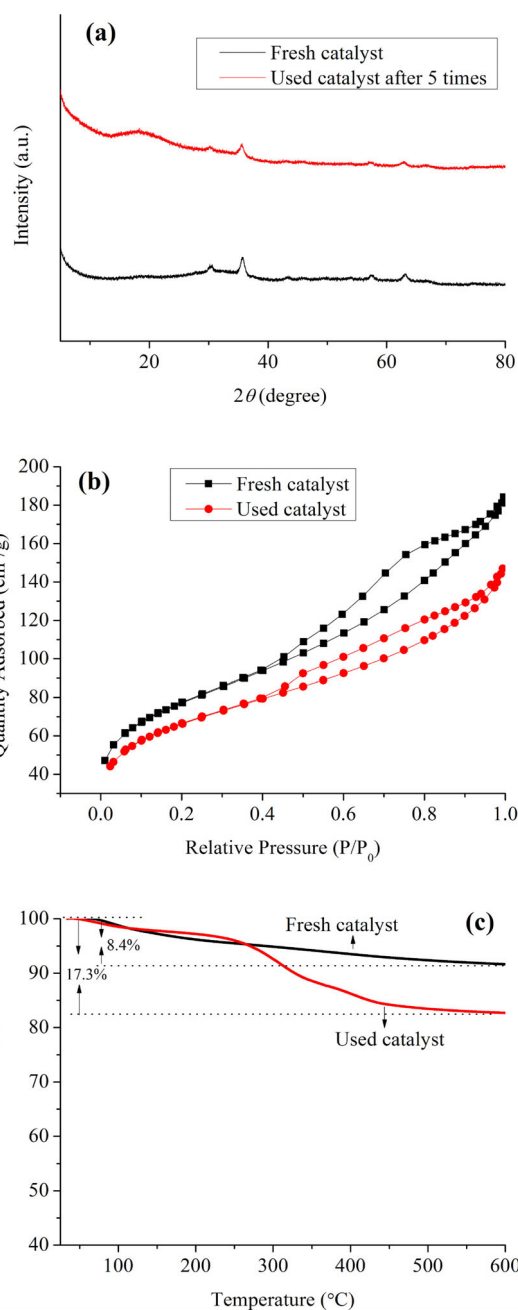


**Figure 7.** (a) XRD patterns, (b)  $N_2$  adsorption–desorption isotherms and (c) TG curves of fresh  $\text{Al}_7\text{Zr}_3@Fe_3O_4(1/1)$  and used  $\text{Al}_7\text{Zr}_3@Fe_3O_4(1/1)$  catalysts, respectively, after five reaction runs.

be reused several times under the applied reaction conditions without significant decline in catalytic activity. Additionally, the  $\text{Al}_7\text{Zr}_3@Fe_3O_4(1/1)$  catalyst was found to exhibit good feasibility for CTH of alternative biomass-derived furanic aldehydes. It is envisaged that the developed low-cost, efficient, durable, and easily-separated catalyst holds a promising potential for CTH of biomass-derived molecules.

**Table 3.** CTH of alternative biomass-derived aldehydes over  $\text{Al}_7\text{Zr}_3@Fe_3O_4$ .<sup>[a]</sup>

Entry	Substrate	Product	Temp. [°C]	Time [h]	Conv. [%]	Yield [%]
1 <sup>[b]</sup>			180	4	93.6	80.5
2			180	4	82.7	71.0
3			180	6	> 99	70.6 <sup>[c]</sup> / 23.2 <sup>[d]</sup>

[a] Reaction conditions: Substrate (2 mmol), 2-propanol (10 mL),  $\text{Al}_7\text{Zr}_3@Fe_3O_4$ (1/1) catalyst (0.08 g). [b] 0.06 g  $\text{Al}_7\text{Zr}_3@Fe_3O_4$ (1/1) catalyst. [c] Yield of 2,5-furandimethanol. [d] Yield of HMF.

## Experimental Section

### Materials

$\text{Fe}(\text{NO}_3)_3 \cdot 9\text{H}_2\text{O}$  ( $\geq 98\%$ ) and  $\text{Al}(\text{NO}_3)_3 \cdot 9\text{H}_2\text{O}$  (98%) were purchased from Riedel-de Haen,  $\text{FeCl}_2 \cdot 4\text{H}_2\text{O}$  ( $\geq 99\%$ ) from Merck, and  $\text{ZrOCl}_2 \cdot 8\text{H}_2\text{O}$  ( $\geq 99\%$ ) and furfural (FF,  $\geq 99\%$ ) from Fluka. Ammonium hydroxide solution (25–28%  $\text{NH}_3$  basis), poly(ethylene glycol) ( $M_{\text{average}} = 2000$ ), FAOL (98%), 5-methylfurfural (99%), 2-propanol (99.5%), ethanol (99.5%), acetone ( $\geq 99\%$ ), and naphthalene ( $> 99\%$ , internal standard) were procured from Sigma-Aldrich. 5-hydroxymethylfurfural (HMF,  $\geq 95\%$ ), 2,5-furandicarboxaldehyde ( $\geq 95\%$ ), 5-methylfuran-2-methanol ( $\geq 95\%$ ), and 2,5-furandimethanol ( $\geq 95\%$ ) were provided by Bepham Ltd.

### Catalyst preparation

The  $\text{Fe}_3\text{O}_4$  catalyst support particles were synthesized by a facile coprecipitation method.<sup>[38]</sup> Briefly,  $\text{Fe}(\text{NO}_3)_3 \cdot 9\text{H}_2\text{O}$  (6 mmol) and  $\text{FeCl}_2 \cdot 4\text{H}_2\text{O}$  (3 mmol) were dissolved in deionized water (50 mL) under nitrogen at room temperature, and then poly(ethylene glycol) (1 g) was added to the solution to prevent the magnetic particles from aggregating during the following generation process.<sup>[39]</sup> Afterwards, the resulting solution was stirred at 85 °C (oil bath) for 15 min, and ammonium hydroxide solution was dropwise added under vigorous stirring until pH 9 was reached (black slurry) followed by continued stirring for another 30 min at 85 °C. Subsequently, the black  $\text{Fe}_3\text{O}_4$  particles were collected by the use of a permanent external magnet, washed to neutral pH with deionized water, and left in deionized water (150 mL) until they were used for catalyst preparation.

A series of  $\text{Al}_7\text{Zr}_3@Fe_3O_4$  catalysts with different ratios of  $\text{Al}_7\text{Zr}_3$  (Al/Zr molar ratio = 7:3) and  $\text{Fe}_3\text{O}_4$  were prepared through a coprecipitation method at room temperature.<sup>[23]</sup> Firstly, the as-synthesized  $\text{Fe}_3\text{O}_4$  particles (3 mmol) were dispersed into aqueous  $\text{Al}^{3+}/\text{Zr}^{4+}$  solution (200 mL; 7.88 g  $\text{Al}(\text{NO}_3)_3 \cdot 9\text{H}_2\text{O}$ , 21 mmol; 2.90 g  $\text{ZrOCl}_2 \cdot 8\text{H}_2\text{O}$ , 9 mmol) with ultrasonication for 30 min. Then, the pH value of the suspension was adjusted to 9 by slow addition of ammonium hydroxide solution followed by stirring for another 5 h. Afterwards, the precipitate was collected by using a permanent external magnet, washed thoroughly with deionized water until neutral pH following dried at 80 °C overnight. Finally, the dried precipitate was calcined at 300 °C under nitrogen atmosphere for 4 h resulting in the catalyst henceforth referred to as  $\text{Al}_7\text{Zr}_3@Fe_3O_4$ (1/1). Analogous  $\text{Al}_7\text{Zr}_3@Fe_3O_4$ (2/1) and  $\text{Al}_7\text{Zr}_3@Fe_3O_4$ (1/2) catalysts were prepared

based on the above procedure using 42/18/3 mmol and 21/9/6 mmol of  $\text{Al}^{3+}/\text{Zr}^{4+}/\text{Fe}_3\text{O}_4$ , respectively. Also, references of pure  $\text{Al}_7\text{Zr}_3$  (Al-Zr mixed oxide) and  $\text{Fe}_3\text{O}_4$  were prepared by the described coprecipitation method.

### Catalyst characterization

Powder X-ray diffraction (XRD) measurements were conducted on a Huber G670 diffractometer with  $\text{Cu}_{K\alpha}$  radiation at room temperature in the  $2\theta$  interval 5–80°. Element mapping were obtained by energy-dispersive X-ray analysis from a Quanta 200 ESEM FEG operated at 10 kV. TEM images were provided using a FEI Tecnai microscope operated at 200 kV.  $\text{N}_2$  physisorption experiments were performed at –196 °C with a Micromeritics ASAP 2020 instrument. Before the  $\text{N}_2$  physisorption measurements, all samples were degassed in vacuum at 200 °C for 4 h. The specific surface areas of as-prepared materials were measured by the BET method, and mean pore sizes were evaluated by the Barrett-Joyner-Halenda (BJH) method. XRF tests were performed using a PANalytical Epsilon3-XL analyzer with standard addition method. Firstly, the sample was dissolved in acidic solution containing  $\text{HNO}_3$  and  $\text{H}_2\text{SO}_4$ , then diluted into 10 mL and hereof 0.5 mL solution dispersed in 0.5 g  $\text{TiO}_2$ . After fully mixing, the mixed sample was dried at 100 °C and then directly measured. The magnetization data were acquired in hysteresis mode at 17 °C by using a Quantum-Design MPMS-XL SQUID magnetometer. TGA was fulfilled under a dynamic air atmosphere (30  $\text{mL min}^{-1}$ ) using a METTLER TOLEDO thermal analyzer in the temperature interval 25–600 °C with a constant heating rate of 10 °C  $\text{min}^{-1}$ .  $\text{NH}_3/\text{CO}_2$ -TPD were performed on a Micromeritics AutoChem II 2920 apparatus. The sample (50 mg) was firstly degassed at 300 °C for 1 h under helium flow (25  $\text{mL min}^{-1}$ ), cooled down to 50 °C followed by purging with  $\text{NH}_3/\text{CO}_2$ -He mixture gas flow (15  $\text{mL min}^{-1}$ ) for 1 h. After flushing with high-purity He for additional 1 h to remove the remaining and weakly adsorbed  $\text{NH}_3$  or  $\text{CO}_2$ ,  $\text{NH}_3/\text{CO}_2$  TPD profiles were subsequently recorded by increasing the temperature from 50 to 300 °C with a heating rate of 10 °C  $\text{min}^{-1}$  under pure He flow and maintaining this temperature for additionally 1 h. ICP-OES analysis was completed on a PerkinElmer Optima 8000 equipment on filtrates after catalyst removing by an external magnet to examine the leaching of metal species upon catalyst reuse.

### CTH and product analysis

CTH of FF was performed in a 50 mL stainless-steel autoclave containing a magnetic stirring bar. Typically, FF (0.1922 g, 2 mmol), 2-propanol (10 mL), and catalyst (0.04 g) were charged into the reactor, which was then sealed and heated to a designed temperature for an intended reaction time. Time zero of the experiments was considered when the reaction temperature reached the target temperature occurring at 120, 140, 160 and 180 °C after 20, 22, 26 and 30 min, respectively. After completion of the reaction, the reactor was rapidly cooled to room temperature in a cold water bath.

Identification of liquid products in the reaction mixture was achieved by GC-MS (Agilent 6850-5975C) equipped with HP-5MS capillary column (30.0 m  $\times$  250  $\mu\text{m}$   $\times$  0.25  $\mu\text{m}$ ). The reactant and product samples were quantitatively analyzed on the basis of standard curves with commercial samples using naphthalene as internal standard on a GC (Agilent 6890 N) equipped with FID detector and HP-5MS capillary column (30.0 m  $\times$  250  $\mu\text{m}$   $\times$  0.25  $\mu\text{m}$ ). The

temperature program used in the analysis was 60 °C for 1 min followed by heating to 230 °C with a heating ramp of 10 °C min<sup>-1</sup> and hold for 4 min.

## Acknowledgements

J.H. thank the Chinese State Scholarship Fund (No. 201606670008) for financial support of the work, and acknowledge the Department of Chemistry, Technical University of Denmark for support.

## Conflict of interest

The authors declare no conflict of interest.

**Keywords:** aldehydes · alcohols · biomass · hydrogenation · magnetic properties

- [1] D. M. Alonso, S. G. Wettstein, J. A. Dumesic, *Chem. Soc. Rev.* **2012**, *41*, 8075–8098.
- [2] M. J. Gilkey, B. Xu, *ACS Catal.* **2016**, *6*, 1420–1436.
- [3] H. Li, Z. Fang, R. L. Smith, Jr., S. Yang, *Prog. Energy Combust. Sci.* **2016**, *55*, 98–194.
- [4] H. Li, S. Saravanamurugan, S. Yang, A. Riisager, *Green Chem.* **2016**, *18*, 726–734.
- [5] S. Saravanamurugan, A. Riisager, E. Taarning, S. Meier, *Chem. Commun.* **2016**, *52*, 12773–12776.
- [6] R. Mariscal, Maireles-P. Torres, M. Ojeda, I. Sádaba, M. L. Granados, *Energy Environ. Sci.* **2016**, *9*, 1144–1189.
- [7] H. Li, S. Yang, A. Riisager, A. Pandey, R. S. Sangwan, S. Saravanamurugan, R. Luque, *Green Chem.* **2016**, *18*, 5701–5735.
- [8] M. Audemar, C. Ciotonea, K. D. O. Vigier, S. Royer, A. Ungureanu, B. Dragoi, E. Dumitriu, F. Jérôme, *ChemSusChem* **2015**, *8*, 1885–1891.
- [9] A. Corma, S. Iborra, A. Velty, *Chem. Rev.* **2007**, *107*, 2411–2502.
- [10] F. H. Isikgor, C. R. Becer, *Polym. Chem.* **2015**, *6*, 4497–4559.
- [11] D. M. Alonso, S. G. Wettstein, J. A. Dumesic, *Green Chem.* **2013**, *15*, 584–595.
- [12] M. Li, Y. Hao, Cárdenas-F. Lizana, M. A. Keane, *Catal. Commun.* **2015**, *69*, 119–122.
- [13] S. T. Thompson, H. H. Lamb, *ACS Catal.* **2016**, *6*, 7438–7447.
- [14] Q. Yuan, D. Zhang, L. van Haandel, F. Ye, T. Xue, *J. Mol. Catal. A* **2015**, *406*, 58–64.
- [15] S. Sitthitha, T. Sooknoi, Y. Ma, P. B. Balbuena, D. E. Resasco, *J. Catal.* **2011**, *277*, 1–13.
- [16] R. V. Sharma, U. Das, R. Sammynaiken, A. K. Dalai, *Appl. Catal. A* **2013**, *454*, 127–136.
- [17] M. Grasemann, G. Laurenczy, *Energy Environ. Sci.* **2012**, *5*, 8171–8181.
- [18] R. Bigler, R. Huber, M. Stöckli, A. Mezzetti, *ACS Catal.* **2016**, *6*, 6455–6464.
- [19] H. Li, Z. Fang, S. Yang, *ACS Sustainable Chem. Eng.* **2016**, *4*, 236–246.
- [20] M. Chia, J. A. Dumesic, *Chem. Commun.* **2011**, *47*, 12233–12235.
- [21] L. Bui, H. Luo, W. R. Gunther, Román-Y. Leshkov, *Angew. Chem. Int. Ed.* **2013**, *52*, 8022–8025; *Angew. Chem.* **2013**, *125*, 8180–8183.
- [22] X. Tang, H. Chen, L. Hu, W. Hao, Y. Sun, X. Zeng, L. Lin, S. Liu, *Appl. Catal. B* **2014**, *147*, 827–834.
- [23] J. He, H. Li, Y. Lu, Y. Liu, Z. Wu, D. Hu, S. Yang, *Appl. Catal. A* **2016**, *510*, 11–19.
- [24] J. Song, B. Zhou, H. Zhou, L. Wu, Q. Meng, Z. Liu, B. Han, *Angew. Chem.* **2015**, *127*, 9531–9535.
- [25] J. He, H. Li, Y. Liu, W. Zhao, T. Yang, W. Xue, S. Yang, *J. Ind. Eng. Chem.* **2016**, *43*, 133–141.
- [26] A. H. Valekar, K. Cho, S. K. Chitale, D. Hong, G. Cha, U. Lee, D. W. Hwang, C. Serre, J. Chang, U. K. Hwang, *Green Chem.* **2016**, *18*, 4542–4552.
- [27] J. R. Ruiz, C. Jiménez-Sanchidrián, *Curr. Org. Chem.* **2007**, *11*, 1113–1125.
- [28] M. Koehle, R. F. Lobo, *Catal. Sci. Technol.* **2016**, *6*, 3018–3026.
- [29] J. Li, J. Liu, H. Zhou, Y. Fu, *ChemSusChem* **2016**, *9*, 1339–1347.
- [30] Z. Gao, L. Yang, G. Fan, F. Li, *ChemCatChem* **2016**, *8*, 3769–3779.
- [31] H. Li, J. He, A. Riisager, S. Saravanamurugan, B. Song, S. Yang, *ACS Catal.* **2016**, *6*, 7722–7727.
- [32] J. Guo, S. Zhu, Y. Cen, Z. Qin, J. Wang, W. Fan, *Appl. Catal. B* **2017**, *200*, 611–619.
- [33] F. Chambon, F. Rataboul, C. Pinel, A. Cabiac, E. Guillon, N. Essayem, *Appl. Catal. B* **2011**, *105*, 171–181.
- [34] E. Pighin, V. K. Diez, J. I. D. Cosimo, *Appl. Catal. A* **2016**, *517*, 151–160.
- [35] C. Yue, G. Li, E. A. Pidko, J. J. Wiesfeld, M. Rigutto, E. J. M. Hensen, *ChemSusChem* **2016**, *9*, 2421–2429.
- [36] C. Opris, B. Cojocaru, N. Gheorghie, M. Tudorache, S. M. Coman, V. I. Parvulescu, B. Duraki, F. Krumeich, J. A. van Bokhoven, *J. Catal.* **2016**, *339*, 209–227.
- [37] H. H. T. Vu, T. S. Atabaev, N. D. Nguyen, Y. Hwang, H. Kim, *J. Sol-Gel Sci. Technol.* **2014**, *71*, 391–395.
- [38] M. Wang, G. Fang, P. Liu, D. Zhou, C. Ma, D. Zhang, J. Zhan, *Appl. Catal. B* **2016**, *188*, 113–122.
- [39] J. M. Rubio-Caballero, S. Saravanamurugan, P. Maireles-Torres, A. Riisager, *Catal. Today* **2014**, *234*, 233–236.

Manuscript received: August 1, 2017

Revised manuscript received: September 6, 2017

Accepted manuscript online: ■■■■■, 0000

Version of record online: ■■■■■, 0000

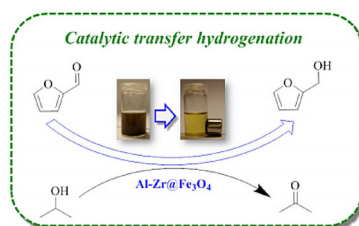
## FULL PAPERS

J. He, H. Li, A. Riisager,\* S. Yang\*

■■ - ■■



### Catalytic Transfer Hydrogenation of Furfural to Furfuryl Alcohol with Recyclable Al-Zr@Fe<sub>3</sub>O<sub>4</sub> Mixed Oxides



**Magnetic hydrogenation:** The bifunctional Al-Zr@Fe<sub>3</sub>O<sub>4</sub> catalyst shows excellent catalytic performance in the catalytic transfer hydrogenation of furfural and other biomass-derived furanic aldehydes using alcohol as hydrogen donor and offers facile reuse in consecutive reactions after its easy recovery by an external magnet.